Asymptotic and leading "correction-to-scaling" susceptibility critical exponents and amplitudes for ferromagnets with quenched disorder

S. N. Kaul
School of Physics, University of Hyderabad, Central University Post Office, Hyderabad 500 134, Andhra Pradesh, India and Institut für Physik, Max-Planck-Institut für Metallforschung, Heisenbergstrasse 1, 7000 Stuttgart 80, West Germany*
(Received 5 January 1988)

Accurate values of the asymptotic susceptibility critical exponent (γ), critical amplitude (Γ), and the leading "correction-to-scaling" exponents and amplitudes for quench-disordered ferromagnets have been determined for the first time through an elaborate analysis of precise and comprehensive ac susceptibility data taken on amorphous $Fe_xNi_{80-x}B_{19}Si_1$ ($x=10$, 13, and 16) alloys in the critical region. Consequently, the present work provides unambiguous experimental verification of theoretical predictions based on renormalization-group (RG) calculations, and testifies to their correctness by demonstrating that the exponent γ of the ordered three-dimensional Heisenberg ferromagnet is not affected by the presence of quenched disorder and that the "frozen" disorder plays the role of an irrelevant scaling field (in the RG sense).

I. INTRODUCTION

Considerable efforts devoted to the understanding of critical phenomena in spin systems with quenched disorder during the past decade have not been able to pinpoint[1] the role played by quenched or "frozen" disorder in affecting the critical behavior of pure (ordered) three-dimensional (3D) Heisenberg ferromagnets. Theoretical views on this subject are divided, as is evident from the following remarks. Early high-temperature series-expansion (HT) treatment[2] of the quenched random site-diluted Heisenberg model yielded an anomalous dependence of the susceptibility critical exponent γ on the concentration, x, i.e., for x near 1, γ appeared to increase rapidly from its pure value ($\gamma \simeq 1.4$) and to attain a value as high as 2.5 at a concentration well above the percolation threshold, x_c. Later Brown *et al.*[3] applied the HT method to a quenched random bond-diluted Heisenberg model and found that γ retains its pure value even for concentrations close to x_c. On the other hand, some of the existing renormalization group (RG) calculations[4-7] (henceforth referred to as "conventional" theories), based on the random-exchange Heisenberg model (REHM), which includes both quenched random site- and bond-diluted Heisenberg models, indicate that the critical properties of a pure spin system, for which the specific-heat critical exponent α_p is negative, are unaffected by the presence of short-ranged quenched disorder. A special RG treatment[8] of REHM (henceforth referred to as "unconventional" theory), on the other hand, predicts that the values of critical exponents for the 3D spin system with $\alpha_p < 0$ depend on the amount of quenched disorder present; in the weak-disorder limit, *crossover* to new exponents occurs at $\varepsilon\,[=(T-T_c)/T_c] \approx 10^0$ whereas for x close to x_c (strong-disorder limit) the exponents assume their limiting values (which are close to the Fisher-renormalized tricritical exponent values but considerably larger than the pure ones) over a wide temperature range,[9] e.g., for $x \approx x_c$, $\gamma \approx 2.0$ from $\varepsilon \simeq 10^2$ down to $\varepsilon \simeq 10^{-8}$. The situation on the experimental side is no better and has been mainly complicated by a large scatter[10] in the values of critical exponents reported for amorphous ferromagnets (e.g., values of the susceptibility critical exponent γ scatter between 1.1 and 1.75 whereas $\gamma = 1.386$ for the ordered 3D Heisenberg ferromagnet). A critical evaluation[11] of the experimental techniques and methods of data analysis, employed in the literature to arrive at the reported exponent values, has revealed that the observed scatter can be traced back to one or more of the following serious problems. (i) Extrapolation to zero magnetic field (H), required in the asymptotic analysis[11] (AA) to estimate "zero-field" quantities like spontaneous magnetization (M_s) and initial susceptibility (χ_0) from the magnetization (M) data taken in finite external fields, introduces errors[12] due to the nonlinearity of the $M^{1/\beta}$ versus $(H/M)^{1/\gamma}$ isotherms. (ii) In the scaling-equation-of-state (SES) analysis,[11] systematic uncertainties result from the choice of the magnetic equation of state and the presence of numerous free fitting parameters. (iii) Due attention has not been paid to the important fact that a given analysis, while covering as wide a range of reduced temperature, ε, as possible, should nevertheless be restricted to data that are free from specious but noncritical effects and provide both lower and upper bounds to the temperature range over which a meaningful asymptotic critical exponent may be extracted. (iv) Independent of the method of analysis, it is imperative that in a given experiment a wide range in reduced temperature, particularly in the immediate vicinity of the Curie temperature, T_c, is sampled and the relative error in T_c is small.

Frequent oversight of the problems (iii) and (iv), in particular, has resulted in *average* rather than *asymptotic* exponents in a large number of cases. Thus an unambiguous experimental verification of the theoretical predictions is possible only when the uncertainties resulting from the above-mentioned problems are minimized as far

as possible through a judicious choice of the experimental technique and a careful data analysis. So far as a precise determination of the exponent γ is concerned, uncertainties arising from (i) and (ii) can be completely eliminated in an ac susceptibility (ACS) measurement, which is the most direct and accurate method[11] of determining $\chi_0(T)$, whereas the problems (iii) and (iv) can be successfully tackled through highly accurate measurements and an elaborate data analysis.

II. RELEVANT THEORETICAL CONCEPTS: BRIEF RESUME

Within the framework of the linearized renormalization-group theory,[13,14] the two-point correlation function, in its most general form, can be written as

$$G(\mathbf{R},\varepsilon,H,\{h_k\})\approx R^{-(d-2+\eta)}\tilde{G}(R\varepsilon^{\nu},RH^{\nu/\Delta},\{h_k\varepsilon^{-\nu\lambda_k}\}), \tag{1}$$

where R is the spatial separation, $\varepsilon=(T-T_c)/T_c$ is the reduced separation in temperature from the critical point, T_c, d is the spatial dimensionality, H is the ordering (magnetic) field, $\{h_k\}$ are other relevant ($\lambda_k>0$) and/or irrelevant ($\lambda_k<0$) fields, λ_k are related to the eigenvalues Λ_k of the linear renormalization operator L as $LQ_k=\Lambda_kQ_k=b^{\lambda_k}Q_k$ (note that λ_k are independent of the choice of the rescaling factor b), $\Delta=(2+\gamma-\alpha)/2$ and ν are the gap and spin-spin correlation length exponents, respectively, and $\tilde{G}(x,y,\ldots)$ is the generalized scaling function. The spatial moments of the pair correlation function (1) can then be calculated using the well-known relation

$$\begin{aligned}\mu_m&\equiv\int d^dR\ |R|^mG(\mathbf{R})\\&\approx\int d^dR\ R^{-(d-1)}R^{m+1-\eta}\tilde{G}(R\varepsilon^{\nu},RH^{\nu/\Delta},\{h_k\varepsilon^{-\nu\lambda_k}\})\\&=\frac{2\pi^{d/2}}{\Gamma(d/2)}\int_0^{\infty}dR\ R^{m+1-\eta}\tilde{G}(R\varepsilon^{\nu},RH^{\nu/\Delta},\{h_k\varepsilon^{-\nu\lambda_k}\}).\end{aligned}$$

By dropping the numerical factors and changing the integration variable to $\omega=R\varepsilon^{\nu}$ in the integral, one obtains the result

$$\begin{aligned}\mu_m&\approx\varepsilon^{-\nu(m+2-\eta)}\int_0^{\infty}d\omega\,\omega^{m+1-\eta}\\&\qquad\times\tilde{G}(\omega,\omega H^{\nu/\Delta}/\varepsilon^{\nu},\{h_k\varepsilon^{-\nu\lambda_k}\})\\&\approx\varepsilon^{-[(2-\eta)\nu+m\nu]}\tilde{D}_m(H/\varepsilon^{\Delta},\{h_k/\varepsilon^{\nu\lambda_k}\}).\end{aligned} \tag{2}$$

According to the fluctuation-dissipation theorem, in the vicinity of the critical point, the magnetic susceptibility, χ, and spin-spin correlation function are related through the zeroth-moment expression, i.e., $\chi=\mu_0=\int d^dR\ G(\mathbf{R})$. In view of Eq. (2), such a relation between χ and $G(\mathbf{R})$ implies that

$$\chi(\varepsilon,H,\{h_k\})\approx\varepsilon^{-\gamma}\tilde{D}_0(H/\varepsilon^{\Delta},\{h_k/\varepsilon^{\nu\lambda_k}\}) \tag{3}$$

with the susceptibility exponent γ defined as $\gamma=(2-\eta)\nu$. Next, let us address ourselves to the question: what is the effect of the *relevant* and *irrelevant* scaling fields on the "zero-field" susceptibility, χ_0? If only the relevant scaling fields are present and $H=0$, Eq. (3) reduces to

$$\chi_0(\varepsilon,\{g_k\})=\chi(\varepsilon,0,\{g_k\})\approx\varepsilon^{-\gamma}X(\{g_k\}/\varepsilon^{\{\phi_k\}}), \tag{4}$$

where a new exponent $\phi_k=\nu\lambda_k$, associated with every scaling field $g_k\equiv h_k$, eigenoperator Q_k pair, i.e. (g_k,Q_k), has been introduced. Since for the case under consideration $\{\phi_k\}>0$, the reduced scaling fields $\{\bar{g}_k\}=\{g_k\}/\varepsilon^{\{\phi_k\}}$ are small for temperatures far from the critical point (in a sense $\{g_k\}$ are normalized according to distance from the critical point), start making their presence felt at crossover temperatures $\{\varepsilon_k^*\}\sim\{g_k\}^{1/\{\phi_k\}}$ and as the temperature approaches the critical point $\{\bar{g}_k\}$ become very large so that the perturbation treatment breaks down. The true asymptotic behavior as $\varepsilon\to0$, therefore, certainly differs from the one corresponding to $\{g_k\}=0$ and depends on the nature of the eigenoperator Q_k. The crossover scaling function, $X(z)$, describes the changeover from the pure ($\{g_k\}=0$) critical behavior at temperatures far from the critical point to the *new* critical behavior at temperatures in the immediate vicinity of T_c and its actual shape determines how slow or how fast the actual crossover occurs. Furthermore, Eq. (4) asserts that the shift in the critical temperature, $[T_c(g_k)-T_c(0)]/T_c(0)$, is proportional to g_k^{1/ϕ_k}. Another interesting case arises when all the relevant fields are zero but the irrelevant scaling fields have a finite magnitude. Since λ_k are all negative in this case, the reduced scaling fields $\{\bar{h}_k\}=\{h_k/\varepsilon^{\nu\lambda_k}\}$ tend to zero as $\varepsilon\to0$. For temperatures close to the critical point, the generalized scaling function $\tilde{D}_0(x,y)$ in Eq. (3) can, therefore, be expanded about $r_k=h_k\varepsilon^{\nu|\lambda_k|}=0$ for all k with the result

$$\chi(\varepsilon,H,\{h_k\})\approx\varepsilon^{-\gamma}\tilde{D}(H/\varepsilon^{\Delta})\left[1+\sum_k h_k\varepsilon^{\nu|\lambda_k|}\left.\frac{\partial\tilde{D}_0}{\partial r_k}\right|_{\{r_k=0\}}+\frac{1}{2}\sum_{i,j}h_ih_j\varepsilon^{\nu|\lambda_i|}\varepsilon^{\nu|\lambda_j|}\left.\frac{\partial^2\tilde{D}_0}{\partial r_i\partial r_j}\right|_{\{r_i=r_j=0\}}+\cdots\right],$$

where $\tilde{D}(H/\varepsilon^{\Delta})=\tilde{D}_0(H/\varepsilon^{\Delta},\{r_k=0\})$. In the absence of ordering field, the above expression yields the "zero-field" susceptibility in the form

$$\begin{aligned}\chi(\varepsilon,0,\{h_k\})&=\chi(\varepsilon,0,0)\left[1+\sum_k h_kf_k\varepsilon^{\nu|\lambda_k|}+\frac{1}{2}\sum_{i,j}h_ih_jf_{ij}\varepsilon^{\nu(|\lambda_i|+|\lambda_j|)}+\cdots\right]\\&=\Gamma\varepsilon^{-\gamma}(1+b_{11}\varepsilon^{\Delta_1}+b_{21}\varepsilon^{\Delta_2}+c_{12}\varepsilon^{2\Delta_1}+c_{22}\varepsilon^{2\Delta_2}+\cdots).\end{aligned} \tag{5}$$

In Eq. (5), the zero-field susceptibility in the *pure* case (i.e., when $\{h_k\}=0$), $\chi(\varepsilon,0,0)=\Gamma\varepsilon^{-\gamma}$, Γ is the asymptotic critical amplitude,

$$f_k=\left.\frac{\partial\tilde{D}_0}{\partial r_k}\right|_{\{r_k=0\}},\quad f_{ij}=\left.\frac{\partial^2\tilde{D}_0}{\partial r_i\partial r_j}\right|_{\{r_i=r_j=0\}},$$
$$b_{kl}=\sum_k h_k f_l,\quad c_{jm}=\tfrac{1}{2}\sum_j (h_j)^2 f_m ,$$

the indices l and m denote the first- and second-order derivatives of $\tilde{D}_0$ with respect to r, respectively, and $\Delta_n=\nu\,|\,\lambda_n\,|$. Note that the terms analytic in ε have been omitted in Eq. (5) and $\Delta_1<\Delta_2<\ldots$ because the leading corrections for small ε originate from the least negative λ_k and carry a factor ε^{Δ_k}. Thus the effect of the irrelevant fields is to give rise to corrections to the dominant singular behavior leaving the leading singularity in the asymptotic behavior unaltered (i.e., no crossover from the pure ($\{h_k\}=0$) behavior occurs).

For pure isotropic spin systems with space as well as spin dimensionality of 3 ($d=3$, $n=3$), i.e., for an ordered (crystalline) isotropic 3D nearest-neighbor Heisenberg ferromagnet, the confluent corrections to the susceptibility involve a single exponent Δ [i.e., for such systems, $\Delta_1\equiv\Delta$ and $\Delta_2=0$ in Eq. (5)] only. The HT series-expansion method[15] and RG calculations[16] yield the best theoretical values for the correction exponent[16] Δ and the corresponding correction amplitude[15] μ [$\equiv b_{11}$ in Eq. (5)] for $d=3$, $n=3$ systems as $\Delta=0.550+(-)0.016$ and $\mu=0.45+0.24(-0.17)$, respectively. Introduction of even a small amount of anisotropy, which acts as a relevant scaling field[13] in the RG sense, in such systems results in a crossover to a new critical behavior, whose exact nature depends on the type of anisotropy present.[17] Critical phenomena in quench-disordered spin systems are not as clearly understood as they are in pure (ordered) systems. The main reason for this is that both the applicability and/or accuracy of HT series expansion and the reliability with which the results obtained by RG calculations, based on $\varepsilon(=4-d)$ expansion, on quenched random systems can be extrapolated to $\varepsilon=1$ or 2 ($d=3$ or 2) are a suspect whereas the same techniques (HT and RG) adequately describe the pure critical behavior. The so-called "conventional" RG theories[4-6] demonstrate that the exponent $\phi=\lambda\nu_p$, characterizing the crossover from the pure to the random fixed point, is identically[17] equal to α_p, the specific-heat critical exponent of the pure system, to order ε^2 for $d=2$ and $d=3$ systems so that the pure fixed point is stable against short-ranged quenched disorder only when $\alpha_p<0$ (i.e., for 3D Heisenberg and 3D XY systems) whereas a crossover to random fixed point, which describes a new sharp phase transition characterized by a set of new critical exponents, is expected to occur for systems with $\alpha_p>0$ (3D Ising systems). By contrast, the so-called "unconventional" RG theory,[8] which also employs ε expansion, asserts that in presence of quenched disorder the pure fixed point is not stable even for systems with $\alpha_p<0$, the critical exponents vary continuously[9] with the impurity concentration x and in the extreme disorder limit (as $x\to x_c$), the exponents approach the Fisher-renormalized values (i.e., $\alpha=-1$, $\beta=0.5$, $\gamma=2$, $\delta=5$, $\nu=1$, $\eta=0$) and are independent of the spin dimensionality n. A recent field-theoretical treatment[7] of 2D and 3D quenched random spin systems, which does away with the ε expansion and hence yields more reliable results, confirms all the results of the "conventional" RG theories including the main prediction that the quenched disorder in $n=3,d=3$ spin systems plays the role of an irrelevant scaling field (since $\lambda^H<0$) and as such gives rise to an additional leading confluent correction term in the expression for $\chi_0(\varepsilon)$ that is characterized by the exponent $\Delta_1(=|\lambda^H|\nu_p=|\alpha_p|)$ besides the one present in pure systems and involving the exponent Δ_2 ($=\Delta$), i.e., for 3D-Heisenberg quench disordered systems Eq. (5) takes the form

$$\chi_0(\varepsilon)=\Gamma\varepsilon^{-\gamma}(1+\mu_1\varepsilon^{\Delta_1}+\mu_2\varepsilon^{\Delta_2}) , \tag{6}$$

where only the leading correction terms have been retained, μ_1 ($\equiv b_{11}$) and μ_2 ($\equiv b_{21}$) are the "correction-to-scaling" amplitudes and the exponent Δ_2 ($=\Delta$) has the same value as for the pure system while the exponent Δ_1, which is much smaller in magnitude than Δ_2 and therefore more important, occurs only in the presence of quenched disorder. The best theoretical estimates[7] of the exponents Δ_1 and Δ_2 presently available are $\Delta_1=0.09$ and $\Delta_2=0.48$. These values, however, differ significantly from the expected pure values, i.e., $\Delta_1=|\alpha_p|=0.115$ and $\Delta_2=\Delta=0.55$, because the results of the field-theoretical approach,[7] leading to the above estimates of Δ_1 and Δ_2, are only to second order in the fixed-point coupling.

III. EXPERIMENTAL DETAILS

High-precision (relative accuracy better than 10 ppm) ac susceptibility measurements were performed on amorphous (a-) $Fe_xNi_{80-x}B_{19}Si_1$ ($x=10,13,16$) alloy ribbons, having typical dimensions of $0.04\times2\times20$ mm^3 and prepared by the single-roller technique, at constant temperature values ($\sim$20 mK apart for $T\to T_c$ and $\sim$100 mK for $T\gg T_c$) during both cooling and heating cycles in the reduced-temperature interval $-0.05\le\varepsilon\le0.05$ in the absence and presence of a static magnetic field, H_{dc}, applied parallel to the ac driving field, H_{ac} (both H_{ac} and H_{dc} are directed along the length in the ribbon plane to minimize demagnetizing effects) using LC oscillator[18] ($H_{ac}\simeq5$ mOe and frequency $\nu=15$ kHz) and mutual inductance[19] ($H_{ac}\simeq100$ mOe and $\nu=87$ Hz, and $H_{dc}\simeq1$ Oe) methods. The sample temperature, monitored by a precalibrated platinum resistance sensor in the latter method and by a copper-constantan thermocouple in the former, was, in both cases, kept constant to within ±10 mK during the measurement period at every fixed temperature setting. The coil assembly part of the sample holder was wrapped in a Mu-metal sheet to eliminate the effect of the earth's magnetic field on the ACS measurements. A detailed compositional analysis of the alloy strips used in this work, using JEOL FCS four crystal (wavelength dispersive) spectrometer in conjunction with JSM 35 JEOL scanning electron microscope, revealed

that the change in the Fe concentration, x, over the entire length ($\simeq 2$ cm) of a given ribbon strip did not exceed 0.005 at. % in any case. In view of our earlier finding that within the composition range of present interest T_c varies with x as[20] $dT_c/dx \simeq 26$ K/at. %, the concentration fluctuations in the alloy sample would give rise to a fluctuation in T_c of the order $\delta T_c \simeq 0.13$ K. Therefore, the data taken in the reduced temperature range $\varepsilon \lesssim \delta T_c/T_c$ have not been included in the data analysis.

IV. RESULTS AND DATA ANALYSIS

Magnetic after-effect measurements and ACS data taken in the cooling and heating runs revealed that the domain and hysteresis effects become important for temperatures $(T-T_c) \lesssim 0.1$ K. Data taken in this temperature range have been left out of the analysis. Though the preliminary ACS data on the glassy alloys in question have been reported by us previously,[18] more precise (by an order of magnitude) and exhaustive measurements as well as an elaborate data analysis are presented in this paper. Results of the ACS measurements performed on a-$Fe_xNi_{80-x}B_{19}Si_1$ alloys in zero and finite static magnetic fields are shown in Fig. 1. Note that the susceptibility data presented in this figure have been corrected for demagnetization, i.e., $\chi_0(\varepsilon)=\chi_{\rm meas}(\varepsilon)/[1-N\chi_{\rm meas}(\varepsilon)]$, where the demagnetizing factor N has been determined from the low-field ($\lesssim 20$ Oe) magnetization data taken on the same glassy alloy strips as those used for the present study.

The "conventional" RG theories predict a temperature dependence of the initial susceptibility, $\chi_0(\varepsilon)$, for temperatures ($\varepsilon \gtrsim 0$) not too close to T_c, of the form given by Eq. (6), which includes the leading "correction-to-scaling" confluent singularity terms. Experimentally, however, it is customary to fit $\chi_0(\varepsilon)$ in a finite temperature range near T_c to a pure power law

$$\chi_0(\varepsilon)=\Gamma_{\rm eff}\varepsilon^{-\gamma_{\rm eff}}, \tag{7}$$

where $\Gamma_{\rm eff}$ and $\gamma_{\rm eff}$ are the effective critical amplitude and critical exponent, respectively. This is so because a direct determination of the parameters μ_1, μ_2, Δ_1, and Δ_2 demands a very high precision in the measurements which is often difficult to achieve in practice. For temperatures very close to T_c, a simple relation (see the Appendix) exists between $\gamma_{\rm eff}$ and γ, i.e.,

$$\gamma_{\rm eff}=\gamma-\mu_1\Delta_1\bar{\varepsilon}^{\Delta_1}-\mu_2\Delta_2\bar{\varepsilon}^{\Delta_2}, \tag{8}$$

where $\bar{\varepsilon}$ is a mean reduced temperature of the temperature range covered in the experiment. It is evident from Eq. (8) that (i) the experimentally determined effective exponent $\gamma_{\rm eff}$ may significantly differ from the theoretically predicted asymptotic (universal) exponent γ, and (ii) $\gamma_{\rm eff}(\varepsilon)$, defined as[21] $\gamma_{\rm eff}(\varepsilon)=d[\ln\chi_0^{-1}(\varepsilon)]/d(\ln\varepsilon)$, coincides with γ only in the limit $\varepsilon\to 0+$, i.e., $\gamma=\lim_{\varepsilon\to 0+}[\gamma_{\rm eff}(\varepsilon)]$. Note that $\gamma_{\rm eff}(\varepsilon)$ is a local measure for the degree of singularity of $\chi_0(\varepsilon)$ in the critical region and is given by Eq. (8) with $\bar{\varepsilon}$ replaced by ε. A corresponding relation between $\Gamma_{\rm eff}$ and Γ, obtained by combining Eqs. (7) and (8), and comparing the resulting expression with Eq. (6), is given by

$$\Gamma_{\rm eff}=\Gamma\langle(1+\mu_1\bar{\varepsilon}^{\Delta_1}+\mu_2\bar{\varepsilon}^{\Delta_2})\bar{\varepsilon}^{-(\mu_1\Delta_1\bar{\varepsilon}^{\Delta_1}+\mu_2\Delta_2\bar{\varepsilon}^{\Delta_2})}\rangle_{\rm av}, \tag{9}$$

where $\langle\ \rangle_{\rm av}$ denotes the average over the investigated reduced temperature range.

Equations (7)–(9) demonstrate that a prior knowledge of $\Gamma_{\rm eff}$, $\gamma_{\rm eff}$, and T_c is required for extracting values of Γ, γ, μ_1, μ_2, Δ_1, and Δ_2 from the experimental data. In order to achieve high accuracy in the determination of T_c and $\gamma_{\rm eff}$ (and hence of $\Gamma_{\rm eff}$), the analytical method of Kouvel and Fisher[21] (KF), which is based on the alternative form of Eq. (7), i.e.,

$$X(T)\equiv\chi_0^{-1}(T)[d\chi_0^{-1}(T)/dT]^{-1}$$
$$=(T-T_c)/\gamma_{\rm eff}=\varepsilon(T_c/\gamma_{\rm eff}), \tag{10}$$

is used. According to this method, the $X(T)$ versus T plot in the asymptotic critical region (ACR), where $\chi_0(T)$ can be approximated by a power law [Eq. (7)], is a straight line whose slope is $1/\gamma_{\rm eff}$ and intercept on the T axis yields T_c. Since the $\chi_0(T)$ data points are taken at temperature intervals of ~ 20 mK and the three-point differentiation method is used to evaluate $d\chi_0(T)/dT$, smoothing of the data over a temperature interval ~ 40 mK occurs. Plots of $X(T)$ against ε in Fig. 2 for the investigated glassy alloys demonstrate the validity of Eq. (10) [and hence of Eq. (7)] in a narrow temperature range above T_c. The choice of the parameters T_c and $\gamma_{\rm eff}$ that gives the best least-squares fit to the $X(T)$ data based on Eq. (10) over the specified reduced temperature range is given in Table I. The lower and upper bounds to the temperature range over which these fits are made and the optimal values of the fitting parameters are arrived at by the procedure whose details are given in our earlier report.[18] Values of T_c and $\gamma_{\rm eff}$ so obtained are then used in Eq. (7) to compute the corresponding values of $\Gamma_{\rm eff}$. Data points are noticed to start deviating at a temperature $\varepsilon_{\rm CO}$ (shown in Fig. 2 by downward arrows) from the fitted straight lines and the deviations become more and more

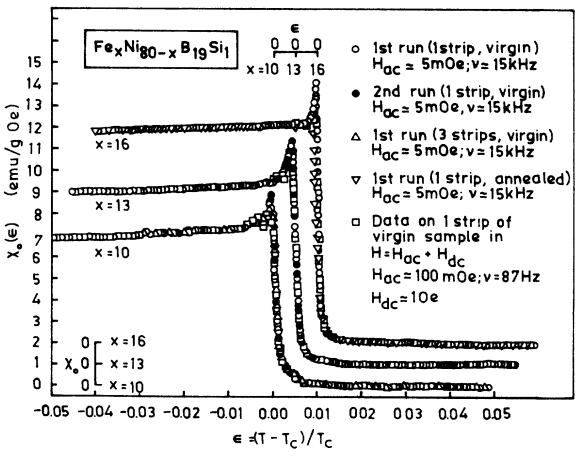

FIG. 1. Initial susceptibility, χ_0, as a function of temperature for amorphous $Fe_xNi_{80-x}B_{19}Si_1$ alloys. Note the change of scale for $x=10$, 13, and 16.

TABLE I. Effective and asymptotic values of the critical exponent and critical amplitude and the "correction-to-scaling" exponents Δ_1,Δ_2 and amplitudes μ_1,μ_2 for amorphous $Fe_xNi_{80-x}B_{19}Si_1$ alloys: Comparison with the corresponding values for crystalline Fe and Ni, and with those predicted by the theory for three-dimensional Ising and Heisenberg ferromagnets. Numbers in the parentheses denote the uncertainty in the least significant figure. Abbreviations: AA, asymptotic analysis (details concerning the AA-I and AA-II methods are given in Ref. 11); ACS, ac susceptibility; BM, bulk magnetization; HT, high-temperature series expansion; KPM, kink-point method; ND, neutron depolarization; PAC, perturbed angular correlation; PW, present work; RG, renormalization group; SES, scaling equation of state.

Material	References and comments	Method	T_c (K)	Range for fit $\varepsilon=10^3(T-T_c)/T_c$	Γ_{eff} (10^{-4} emu/g Oe)	γ_{eff}	Γ (10^{-4} emu/g Oe)	γ	μ_1 [Δ_1]	μ_2 [Δ_2]
$x=10$	11	BM,AA-I	186.50(30)	0.80–35	2.222(7)	1.350(40)				
	11	BM,AA-II	187.00(30)	0.80–35	2.941(13)	1.350(40)				
	PW[a]	ACS,$H_{dc}=0$	187.06(7)	0.82–34	2.890(30)	1.360(22)	2.66(14)	1.388(12)	0.030(10) [0.11(3)]	0.32(4) [0.55(5)]
	PW[b]	ACS,$H_{dc}=0$	187.27(4)	0.79–35	2.070(40)	1.357(18)	1.80(20)	1.386(12)	0.021(3) [0.11(3)]	0.32(4) [0.55(5)]
	PW[c]	ACS,$H_{dc}=0$	186.26(6)	0.75–35	2.908(70)	1.360(20)	2.60(20)	1.386(13)	0.029(11) [0.10(4)]	0.31(5) [0.54(6)]
	PW[d]	ACS,$H_{dc}\neq0$	187.01(5)	0.81–36	2.955(35)	1.359(21)	2.68(22)	1.386(14)	0.031(5) [0.11(4)]	0.32(4) [0.55(5)]
$x=13$	11	BM,AA-I	268.50(20)	0.62–40	1.348(2)	1.350(40)				
	11	BM,AA-II	268.70(20)	0.56–40	1.695(4)	1.350(40)				
	PW[a]	ACS,$H_{dc}=0$	268.62(8)	0.67–41	1.350(35)	1.352(18)	1.15(15)	1.386(11)	0.030(10) [0.11(3)]	0.48(4) [0.55(4)]
	PW[b]	ACS,$H_{dc}=0$	270.90(5)	0.80–38	1.330(40)	1.354(20)	1.10(20)	1.386(10)	0.026(6) [0.11(4)]	0.49(4) [0.55(5)]
	PW[d]	ACS,$H_{dc}\neq0$	268.66(4)	0.72–39	1.300(35)	1.351(19)	1.07(18)	1.386(12)	0.032(8) [0.10(5)]	0.49(5) [0.54(4)]
$x=16$	23	BM,AA-II	341.87(3)	0.39–54	0.945(14)	1.330(30)				
	PW[a]	ACS,$H_{dc}=0$	341.41(6)	0.53–55	0.948(63)	1.328(23)	0.75(15)	1.386(20)	0.068(12) [0.11(4)]	0.63(7) [0.55(5)]
	PW[d]	ACS,$H_{dc}\neq0$	341.67(5)	0.64–57	0.950(25)	1.329(21)	0.77(13)	1.387(18)	0.070(10) [0.10(5)]	0.65(4) [0.55(4)]
	23	BM,AA-II	351.27(5)	0.74–40	0.918(15)	1.330(30)				
	PW[e]	ACS,$H_{dc}=0$	351.62(5)	0.77–40	0.925(40)	1.333(17)	0.76(12)	1.386(20)	0.071(14) [0.11(3)]	0.65(5) [0.55(5)]
Fe	11	BM,KPM	1044.00(200)	0.80–30		1.333				
	24	ND	1045.86(2)	0.15–4		1.330(15)				
Ni	21	BM,AA-I	627.40	4.10–20		1.340(10)				
	11	BM,SES	626.94(1)	0.06–18		1.310(10)				
	11	PAC	632.09(8)	1.00–100		1.310(10)				

TABLE I. (*Continued*).

Material	References and comments	Method	T_c (K)	Range for fit $\varepsilon=10^3(T-T_c)/T_c$	Γ_{eff} (10^{-4} emu/g Oe)	γ_{eff}	Γ (10^{-4} emu/g Oe)	γ	μ_1 [Δ_1]	μ_2 [Δ_2]
3D-Ising	11	HT						1.250(1)		
	16	RG						1.241(2)		
3D-Heisenberg	16[f]	RG						1.386(4)		
									[0.115(9)]	[0.550(16)]
									[0.09]	[0.48]
	7[g]	RG								

[a]ACS measurements on a single strip (2 cm in length) of the "virgin" alloy ribbon coming from the same batch as that previously used for BM measurements; first experimental run.
[b]Second experimental run on the sample used in footnote a. Increased value of T_c in the second run is due to the structural relaxation caused by the heat treatment (to temperatures as high as 400 K) which the specimen underwent during the first run. Note that the values of Γ_{eff}, γ_{eff}, Γ, and γ remain unaltered (within the error limits).
[c]ACS measurements on three strips (each 2 cm in length) of the "as-quenched" alloy ribbon.
[d]ACS data taken in presence of the external dc magnetic field, $H_{\text{dc}} \simeq 1$ Oe, on a single 2 cm long strip of the "virgin" alloy ribbon.
[e]ACS measurements performed on the same sample as that used for our earlier BM measurements. This sample was annealed at 400 K for two hours before the BM and ACS measurements were performed. It is observed that the structural relaxation consequent upon annealing does not have any influence on Γ_{eff}, γ_{eff}, Γ, and γ.
[f]According to the RG theories (Refs. 4–7 and 17) on quench disordered spin systems, the correction exponent $\Delta_1=|\alpha_p|$ whereas Δ_2 retains its pure value for 3D Heisenberg ferromagnet.
[g]Jug (Ref. 7) uses the notation b_k for λ_k so that $\Delta_1=b_1\nu_p$ and $\Delta_2=b_2\nu_p$.

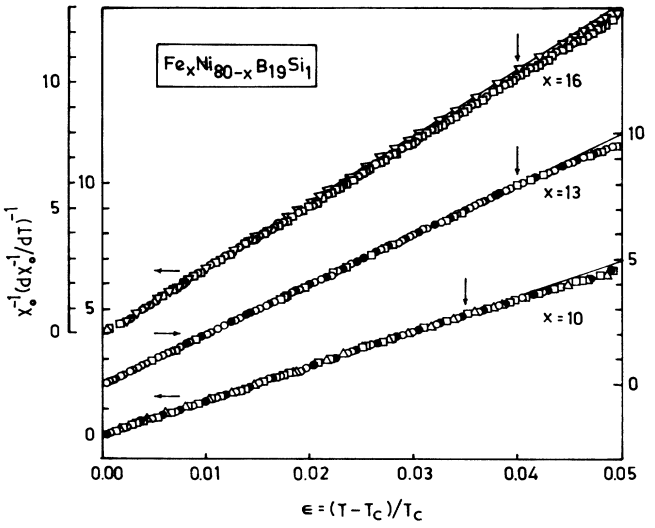

FIG. 2. Temperature dependence of the quantity $\chi_0^{-1}(d\chi_0^{-1}/dT)^{-1}$ for a-Fe$_x$Ni$_{80-x}$B$_{19}$Si$_1$ alloys. Different data symbols in this figure have the same meaning as that indicated in Fig. 1.

pronounced as ε increases beyond ε_{CO}. In view of the definition of $\gamma_{\text{eff}}(\varepsilon)$, i.e.,

$$\gamma_{\text{eff}}(\varepsilon)=d[\ln\chi_0^{-1}(\varepsilon)]/d(\ln\varepsilon)$$
$$=[\chi_0(\varepsilon)d\chi_0^{-1}(\varepsilon)/d\varepsilon]\varepsilon=\varepsilon[T_c/X(T)]\ , \tag{11}$$

this finding implies that $\gamma_{\text{eff}}(\varepsilon)$ increases for $\varepsilon>\varepsilon_{\text{CO}}$. This behavior is now known to be a characteristic[10,11,22] property of amorphous ferromagnets. Additional points that deserve attention are (i) width of the ACR ($\varepsilon\le\varepsilon_{\text{CO}}$) increases with increasing Fe concentration, and (ii) the so-called "crossover temperature," ε_{CO}, shifts to lower temperatures (from 5.5×10^{-2} to 4.0×10^{-2}) for the alloy with $x=16$ as a result of annealing at 400 K for two hours. Both these observations conform well with the results of our earlier magnetization measurements.[10,11,23] Since the behavior of quench disordered ferromagnets in the ACR is the main concern of this paper, the above observations will not be discussed here.

Attempt was first made to extract the values of Γ, γ, μ_1, μ_2, Δ_1, Δ_2, and T_c by fitting $\chi_0(\varepsilon)$ data to Eq. (6) using a nonlinear least-squares fit computer program that treats Γ, γ, μ_1, μ_2,and T_c as free fitting parameters but keeps (Δ_1,Δ_2) pair fixed at a given value in the ranges $0.01\le\Delta_1\le0.20$ and $0.35\le\Delta_2\le0.75$, respectively. The same procedure is repeated for another fixed value of the pair (Δ_1,Δ_2) which differs from the previous value by $(\pm0.01,\pm0.01)$. Best fits, as inferred from the smallest value of the mean square error, are obtained for $\Delta_1=0.10\pm0.05$ and $\Delta_2=0.53\pm0.10$ with the parameter values that have undesirably large uncertainty but are otherwise close to those (determined by the following method) listed in Table I. A substantial reduction in this uncertainty is achieved by decreasing the number of free parameters as follows. Keeping T_c fixed at the value deduced earlier by the KF method (Table I), $\gamma_{\text{eff}}(\varepsilon)$ and

$\Gamma_{\rm eff}(\varepsilon)$ in the ACR are computed for each experimental run from Eqs. (11) and (7), respectively. Accurate values of γ, μ_1, and μ_2 are then given by the choice of these parameters which yields the smallest value of the mean square error (χ^2) when least-squares fits to the $\gamma_{\rm eff}(\varepsilon)$ data are attempted based on Eq. (8) (with $\bar{\varepsilon}$ in this equation replaced by ε; for details see the Appendix) while Δ_1 and Δ_2 are varied in fixed steps of 0.01 within the ranges $0.01 \le \Delta_1 \le 0.20$ and $0.35 \le \Delta_2 \le 0.75$, as mentioned above (note that T_c for all such fits remains constant at the value given by the KF method). The best values of the parameters γ, μ_1, μ_2, Δ_1, and Δ_2 so obtained and listed in Table I are then used to construct the $\Gamma_{\rm eff}(\varepsilon)$ versus

$$[(1+\mu_1\varepsilon^{\Delta_1}+\mu_2\varepsilon^{\Delta_2})\varepsilon^{-(\mu_1\Delta_1\varepsilon^{\Delta_1}+\mu_2\Delta_2\varepsilon^{\Delta_2})}]$$

plot. Consistent with Eq. (9), the straight line through the data points on this plot, obtained by the least-squares method, passes through the origin and its slope is a direct measure of Γ. Figures 3 and 4 serve to demonstrate the typical quality of the least-squares fits to the $\gamma_{\rm eff}(\varepsilon)$ and $\Gamma_{\rm eff}(\varepsilon)$ data based on Eqs. (8) and (9) with the choice of parameters $\Gamma, \gamma, \mu_1, \mu_2, \Delta_1$, and Δ_2 arrived at by the above method. Fits involving only one correction term at a time in Eq. (6) [i.e., when either μ_1 or μ_2 is set equal to zero in Eq. (6)] have also been attempted with the result that the quality of fits, compared to those that take into account both the correction terms, deteriorates, as inferred from the increased value of χ^2, even though the values of Γ and γ remain unaltered (as expected).

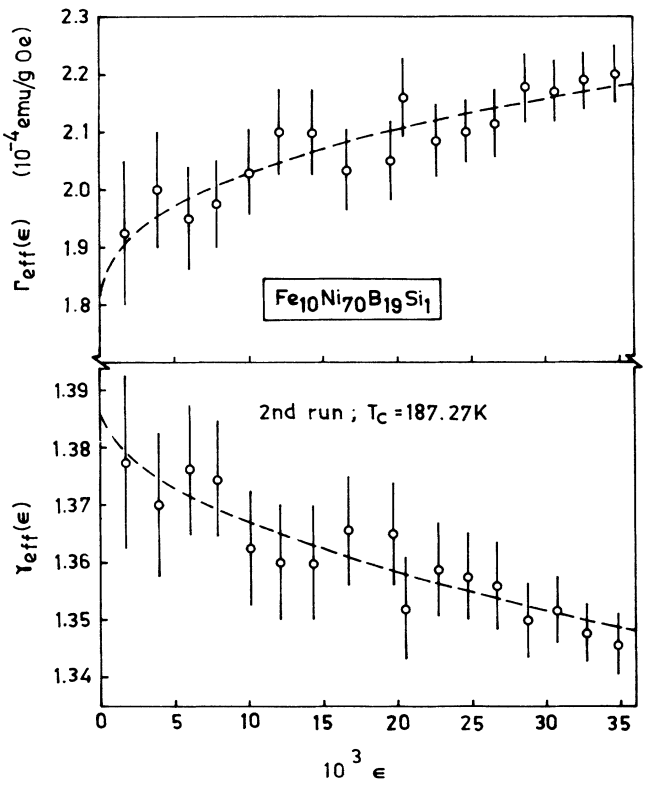

FIG. 3. Variation of the effective critical amplitude, $\Gamma_{\rm eff}(\varepsilon)$, and critical exponent, $\gamma_{\rm eff}(\varepsilon)$, with reduced temperature ε for the glassy alloy $Fe_{10}Ni_{70}B_{19}Si_1$ (second experimental run). Dashed curves denote the result of the least-squares fits to the data based on Eqs. (8) and (9) of the text, while the error limits give the measure of uncertainty in these quantities due to the uncertainty in T_c.

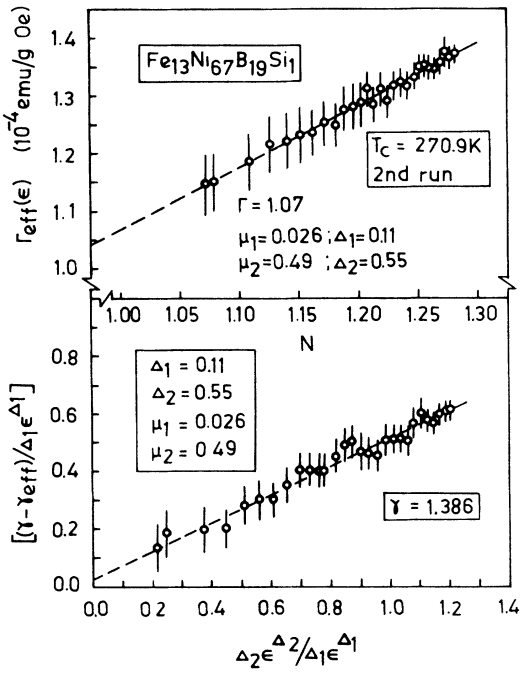

FIG. 4. $\{[\gamma-\gamma_{\rm eff}(\varepsilon)]/\Delta_1\varepsilon^{\Delta_1}\}$ vs $\Delta_2\varepsilon^{\Delta_2}/\Delta_1\varepsilon^{\Delta_1}$ and $\Gamma_{\rm eff}(\varepsilon)$ vs $N \equiv (1+\mu_1\varepsilon^{\Delta_1}+\mu_2\varepsilon^{\Delta_2})\varepsilon^{-(\mu_1\Delta_1\varepsilon^{\Delta_1}+\mu_2\Delta_2\varepsilon^{\Delta_2})}$ plots for amorphous $Fe_{13}Ni_{67}B_{19}Si_1$ (second experimental run) based on the choice of the parameters μ_1, μ_2, Δ_1, Δ_2, γ, and Γ that gives the best least-squares fit of the $\gamma_{\rm eff}(\varepsilon)$ and $\Gamma_{\rm eff}(\varepsilon)$ data to Eqs. (8) and (9) of the text. The dashed straight lines through the data points, obtained by the least-squares method, demonstrate the validity of Eqs. (8) and (9).

V. DISCUSSION

Table I lists the values of the parameters μ_1, μ_2, Δ_1, Δ_2, Γ, γ, and those of T_c, $\Gamma_{\rm eff}$, and $\gamma_{\rm eff}$ obtained by the KF method and compares them with (a) the corresponding effective exponent and amplitude values determined previously[10,11] for the same compositions as the present ones using the modified asymptotic analysis,[11] (b) the $\gamma_{\rm eff}$ values for crystalline ferromagnets[11,24] Fe, Ni, and (c) the values of γ, Δ_1, and Δ_2 predicted by the theory.[7,16] Important points that emerge from this comparison are (i) the KF analysis, Eq. (10), of the ACS data and the asymptotic analysis of the bulk magnetization data yield identical results (values of T_c, $\Gamma_{\rm eff}$, and $\gamma_{\rm eff}$) for the glassy alloys of the same composition and coming from the same batch, (ii) the width of the ACR for γ and the value of $\gamma_{\rm eff}$ are roughly the same in both crystalline and amorphous ferromagnets, (iii) asymptotic critical exponent γ and the "correction-to-scaling" exponents Δ_1 and Δ_2 do

not depend on composition and possess values that are in excellent agreement with those predicted by the "conventional" RG theories,[4–7,17] (iv) by contrast, the correction amplitudes μ_1 and μ_2 are composition-dependent (consistent with the generally accepted thesis that the correction amplitudes, unlike correction exponents, are not universal by themselves but their ratios are); the values of μ_2 determined in the present work fall within the range of values ($0.28 \leq \mu \leq 0.69$) given by the HT series expansion treatment[15] of an isotropic 3D nearest-neighbor spin-infinity Heisenberg model, and (v) exponent γ retains its "pure" value[16] regardless of the alloy composition in the reduced temperature region where, according to the "unconventional" RG theory,[8,9] a crossover to the new exponents ($\gamma \approx 2.0$ is expected[8,9] for the glassy alloys in question as the critical concentration x_c for the appearance of long-range ferromagnetic ordering in the present alloy series is[20] $x_c \simeq 4.9$ at. %) should have already taken place (see Introduction). While observation (i) vindicates the use of the AA method[10,11] to deduce reliable and accurate values of Γ_{eff} and γ_{eff} from the magnetization data taken in finite external fields, observations (ii)–(v) coupled with our earlier finding[10,11] that both the sign and magnitude of the specific heat exponent, α, for the investigated amorphous alloys closely agree with those determined for α in crystalline ferromagnets and with the theoretical value for isotropic nearest-neighbor 3D Heisenberg ferromagnet testify to the validity of the theoretical prediction, based on the "conventional" RG theories, that the critical behavior of ordered $n=3$, $d=3$ spin system with $\alpha_p < 0$ remains unaltered in the presence of quenched disorder.

At this stage, it should be emphasized that some amount of caution has to be exercised while considering the implications of the above-mentioned agreement between theory and experiment, as is evident from the following arguments. In view of the fact that the "conventional" RG theories are based on quenched random site- and/or bond-diluted nearest-neighbor Heisenberg model and that the critical concentrations for bond- and site-percolation for nearest-neighbor exchange interactions on the fcc lattice (which forms an adequate description[25] of the nearest-neighbor atomic configuration in the glassy alloys under consideration) are[1] $p_c^b = 0.119$ and $p_c^s = 0.195$, respectively, whereas for a-$Fe_xNi_{80-x}B_{19}Si_1$ alloy series the percolation concentration[20] is not reached until $p_c \simeq 4.9/80 = 0.061$ (this value exactly matches with the critical concentration for site-percolation on the fcc lattice when the exchange interactions are not confined to the nearest neighbors only but their range extends to third nearest-neighbor distance[1]), we cannot claim to have determined the asymptotic and "correction-to-scaling" exponents and amplitudes for a dilute nearest-neighbor 3D Heisenberg ferromagnet; the parameters of interest in the theory. Note that the longer range of the exchange interactions in the glassy alloys in question has also been previously[25] inferred from bulk magnetization measurements and that Monte Carlo calculations[26] on phase transitions in bond- and site-disordered classical Heisenberg ferromagnets demonstrate that the site disorder is mainly responsible for the concave-upward curvature of $\chi_0^{-1}(T)$ observed in a large number of amorphous ferromagnetic alloys, including the present ones. In the light of the foregoing remarks, the striking agreement between the theoretically predicted and experimentally observed values for the asymptotic and "correction-to-scaling" exponents should be taken to imply that the universality hypothesis, which asserts that the range and type of exchange interaction both are of no consequence so long as the spin-spin correlation length diverges at T_c, is basically correct.

APPENDIX

If $\bar{\varepsilon}$ denotes the mean reduced temperature of the temperature range over which the $\chi_0(\varepsilon)$ data are fitted to a single power law, Eq. (7), and if Γ and γ are also deduced from the $\chi_0(\varepsilon)$ data taken in the same temperature range using Eq. (6) [note that Γ and γ are not expected to depend on the temperature range covered in the experiment, provided this temperature range falls within the asymptotic critical region, since they are the asymptotic values], Eqs. (6) and (7) can be rewritten in the form

$$\chi_0(\bar{\varepsilon}) = \Gamma \bar{\varepsilon}^{-\gamma}(1+\mu_1 \bar{\varepsilon}^{\Delta_1}+\mu_2 \bar{\varepsilon}^{\Delta_2}) , \tag{A1}$$

and

$$\chi_0(\bar{\varepsilon}) = \Gamma_{\text{eff}} \bar{\varepsilon}^{-\gamma_{\text{eff}}} . \tag{A2}$$

A direct relation between γ_{eff} and γ can be obtained by equating the values of

$$d[\ln \chi_0(\bar{\varepsilon})]/d(\ln \bar{\varepsilon}) = \bar{\varepsilon} d[\ln \chi_0(\bar{\varepsilon})]/d\bar{\varepsilon}$$

computed from Eqs. (A1) and (A2), i.e.,

$$\frac{d}{d\bar{\varepsilon}}[\ln(\Gamma_{\text{eff}} \bar{\varepsilon}^{-\gamma_{\text{eff}}})] = \frac{d}{d\bar{\varepsilon}} \ln[\Gamma \bar{\varepsilon}^{-\gamma}(1+\mu_1 \bar{\varepsilon}^{\Delta_1}+\mu_2 \bar{\varepsilon}^{\Delta_2})] .$$

After a few simplifying steps, the following result is arrived at

$$\begin{aligned}
\gamma_{\text{eff}} &= \gamma - (\mu_1 \Delta_1 \bar{\varepsilon}^{\Delta_1}+\mu_2 \Delta_2 \bar{\varepsilon}^{\Delta_2})/(1+\mu_1 \bar{\varepsilon}^{\Delta_1}+\mu_2 \bar{\varepsilon}^{\Delta_2}) \\
&\simeq \gamma - (\mu_1 \Delta_1 \bar{\varepsilon}^{\Delta_1}+\mu_2 \Delta_2 \bar{\varepsilon}^{\Delta_2})(1-\mu_1 \bar{\varepsilon}^{\Delta_1}-\mu_2 \bar{\varepsilon}^{\Delta_2}) \\
&= \gamma - \mu_1 \Delta_1 \bar{\varepsilon}^{\Delta_1} - \mu_2 \Delta_2 \bar{\varepsilon}^{\Delta_2} + \mu_1^2 \Delta_1 \bar{\varepsilon}^{2\Delta_1} \\
&\quad + \mu_1 \mu_2 (\Delta_1 + \Delta_2) \bar{\varepsilon}^{(\Delta_1+\Delta_2)} + \mu_2^2 \Delta_2 \bar{\varepsilon}^{2\Delta_2} .
\end{aligned}$$

Retaining the leading correction terms only, the above expression reduces to

$$\gamma_{\text{eff}} \simeq \gamma - \mu_1 \Delta_1 \bar{\varepsilon}^{\Delta_1} - \mu_2 \Delta_2 \bar{\varepsilon}^{\Delta_2} . \tag{A3}$$

When γ_{eff} in Eq. (A2) is replaced by the right-hand side of Eq. (A3) and the result is equated to the rhs of Eq. (A1), a relation between Γ_{eff} and Γ of the following type is obtained:

$$\Gamma_{\text{eff}} \bar{\varepsilon}^{-\gamma} \cdot \bar{\varepsilon}^{(\mu_1 \Delta_1 \bar{\varepsilon}^{\Delta_1}+\mu_2 \Delta_2 \bar{\varepsilon}^{\Delta_2})} = \Gamma \bar{\varepsilon}^{-\gamma}(1+\mu_1 \bar{\varepsilon}^{\Delta_1}+\mu_2 \bar{\varepsilon}^{\Delta_2}) ,$$

or

$$\Gamma_{\text{eff}} = \Gamma \langle (1+\mu_1 \bar{\varepsilon}^{\Delta_1}+\mu_2 \bar{\varepsilon}^{\Delta_2}) \bar{\varepsilon}^{-(\mu_1 \Delta_1 \bar{\varepsilon}^{\Delta_1}+\mu_2 \Delta_2 \bar{\varepsilon}^{\Delta_2})} \rangle_{\text{av}} , \tag{A4}$$

where $\langle\ \rangle_{av}$ denotes the average over the reduced temperature range covered in the fit. At this stage, it should be emphasized that Eqs. (A3) and (A4) are not only valid for a mean reduced temperature $\bar{\varepsilon}$ but also for any temperature value ε within the temperature range specified in Table I for a given sample primarily because T_c remains practically constant (within the error limits) in this temperature range; the result borne out by the "range-of-fit" analysis. Alternatively, Eqs. (A3) and (A4), without any loss of generality, can be written with $\bar{\varepsilon}$ replaced by ε, i.e.,

$$\gamma_{\text{eff}}(\varepsilon)=\gamma-\mu_1\Delta_1\varepsilon^{\Delta_1}-\mu_2\Delta_2\varepsilon^{\Delta_2}\ ,$$

or

$$[\gamma-\gamma_{\text{eff}}(\varepsilon)]/\Delta_1\varepsilon^{\Delta_1}=\mu_1+\mu_2(\Delta_2\varepsilon^{\Delta_2})/\Delta_1\varepsilon^{\Delta_1}\ , \qquad \text{(A5)}$$

and

$$\Gamma_{\text{eff}}(\varepsilon)=\Gamma(1+\mu_1\varepsilon^{\Delta_1}+\mu_2\varepsilon^{\Delta_2})\varepsilon^{-(\mu_1\Delta_1\varepsilon^{\Delta_1}+\mu_2\Delta_2\varepsilon^{\Delta_2})}\ , \qquad \text{(A6)}$$

where $\gamma_{\text{eff}}(\varepsilon)$ and $\Gamma_{\text{eff}}(\varepsilon)$ are defined by Eq. (11) of the text and the relation $\chi_0(\varepsilon)=\Gamma_{\text{eff}}(\varepsilon)\cdot\varepsilon^{-\gamma_{\text{eff}}(\varepsilon)}$, respectively. The main advantage in using Eqs. (A5) and (A6) instead of Eqs. (A3) and (A4) for determining μ_1, μ_2, Δ_1, Δ_2, Γ, and γ is that the values for these parameters obtained thereby are more reliable because Eqs. (A5) and (A6) contain $\gamma_{\text{eff}}(\varepsilon)$ and $\Gamma_{\text{eff}}(\varepsilon)$ and hence bring out the total uncertainty (including the uncertainty in T_c) in the values of γ_{eff} and Γ_{eff} at each experimentally set value of ε as contrasted with the uncertainty in γ_{eff} and Γ_{eff} at a mean reduced temperature $\bar{\varepsilon}$ of the temperature range covered in a given fit which is bound to be considerably smaller due to the averaging involved in the fitting process.

---

*Permanent address.

[1]R. B. Stinchcombe, in *Phase Transitions and Critical Phenomena,* edited by C. Domb and M. S. Green (Academic, New York, 1983), Vol. 7, p. 151 and references quoted therein; M. Fähnle, J. Magn. Magn. Mater. **59**, 266 (1986).

[2]G. S. Rushbrooke, R. A. Muse, R. L. Stephenson, and K. Pirnie, J. Phys. C **5**, 3371 (1972); G. S. Rushbrooke, G. A. Baker, and P. W. Wood, in *Phase Transitions and Critical Phenomena,* edited by C. Domb and M. S. Green (Academic, New York, 1974), Vol. 3, p. 245.

[3]E. Brown, J. W. Essam, and C. M. Place, J. Phys. C **8**, 321 (1975).

[4]D. E. Khmel'nitzki, Zh. Eksp. Teor. Fiz. **68**, 1960 (1975) [Sov. Phys.—JETP **41**, 981 (1976)]; T. C. Lubensky, Phys. Rev. B **11**, 3573 (1975).

[5]G. Grinstein and A. Luther, Phys. Rev. B **13**, 1329 (1976).

[6]A. Weinrib and B. I. Halperin, Phys. Rev. B **27**, 413 (1983).

[7]G. Jug, Phys. Rev. B **27**, 609 (1983).

[8]G. Sobotta and D. Wagner, J. Magn. Magn. Mater. **49**, 77 (1985), and references cited therein.

[9]G. Sobotta and D. Wagner, J. Magn. Magn. Mater. **15-18**, 257 (1980).

[10]S. N. Kaul, IEEE Trans. Magn. **20**, 1290 (1984), and references quoted therein.

[11]S. N. Kaul, J. Magn. Magn. Mater. **53**, 5 (1985), and references cited therein.

[12]A. Aharoni, J. Magn. Magn. Mater. **58**, 297 (1986); I. Yeung, R. M. Roshko, and G. Williams, Phys. Rev. B **34**, 3456 (1986).

[13]M. E. Fisher, Rev. Mod. Phys. **46**, 597 (1974).

[14]F. J. Wegner, in *Phase Transitions and Critical Phenomena,* edited by C. Domb and M. S. Green (Academic, New York, 1976), Vol. 6, p. 7.

[15]W. J. Camp and J. P. Van Dyke, J. Phys. A **9**, 731 (1976).

[16]L. C. LeGuillou and J. Zinn-Justin, Phys. Rev. B **21**, 3976 (1980).

[17]A. Aharony, in *Phase Transitions and Critical Phenomena,* edited by C. Domb and M. S. Green (Academic, New York, 1976), Vol. 6, p. 357.

[18]S. N. Kaul, A. Hofmann, and H. Kronmüller, J. Phys. F **16**, 365 (1986).

[19]S. N. Kaul and S. Methfessel, Solid State Commun. **47**, 147 (1983).

[20]S. N. Kaul, IEEE Trans. Magn. **17**, 1208 (1981).

[21]J. S. Kouvel and M. E. Fisher, Phys. Rev. **136**, A1626 (1964).

[22]M. Fähnle, G. Herzer, H. Kronmüller, R. Meyer, M. Saile, and T. Egami, J. Magn. Magn. Mater. **38**, 240 (1983).

[23]S. N. Kaul, W.-U. Kellner, and H. Kronmüller, Key Eng. Mater. **13-15**, 669 (1987).

[24]N. Stusser, M. Th. Rekveldt, and T. Spruijt, Phys. Rev. B **31**, 5905 (1985).

[25]S. N. Kaul, Phys. Rev. B **24**, 6550 (1981); **27**, 5761 (1983).

[26]M. Fähnle, J. Magn. Magn. Mater. **45**, 279 (1984); J. Phys. C **18**, 181 (1985).